Aerosol Science and Technology, 38(S1):92–103, 2004

ISSN: 0278-6826 print / 1521-7388 online
DOI: 10.1080/02786820390229507

Measurement of Ambient Aerosol Composition During the PMTACS-NY 2001 Using an Aerosol Mass Spectrometer. Part I: Mass Concentrations

Frank Drewnick,[1] James J. Schwab,[1] John T. Jayne,[2] Manjula Canagaratna,[2] Douglas R. Worsnop,[2] and Kenneth L. Demerjian[1]

[1]*Atmospheric Sciences Research Center, State University of New York, Albany, New York*
[2]*Center for Aerosol and Cloud Chemistry, Aerodyne Research Inc., Billerica, Massachusetts*

Semicontinuous ambient aerosol composition measurements performed during the PMTACS-NY Summer 2001 field campaign in Queens/New York with an aerosol mass spectrometer (AMS, developed by Aerodyne Research Inc.) are described. The measurements include 10 min averages of the nonrefractory sulfate, nitrate, ammonium, chloride, and organic mass concentrations in the particle size range of 50 to approximately 1000 nm. Particle-bound water concentrations (i.e., aerosol liquid water content) were estimated from the mass spectral information and local meteorological data. Aggregate semicontinuous AMS mass measurements were compared with those from a TEOM mass monitor that was also deployed at the PMTACS-NY 2001 site. On average, the AMS observed 64% of the total particulate matter mass measured by the TEOM Monitor. Filter and additional semicontinuous particulate sulfate measurements performed simultaneously at the site suggest that the observed discrepancy in mass balance between the two instruments is attributable to a combination of large particles ($\geq$1 μm) lost in the AMS inlet system and the refractory aerosol components not measured by the AMS. Measured diurnal patterns of sulfate, nitrate, organics, and total nonrefractory mass concentrations indicate that elevated PM levels measured during this campaign were due to regional transport as well as local production of particulate matter.

Received 2 February 2003; accepted 13 March 2003.

This work was supported in part by the New York State Energy Research and Development Authority (NYSERDA), contract # 4918ERTERES99; the U.S. Environmental Protection Agency (EPA), cooperative agreement # R828060010; and New York State Department of Environmental Conservation (NYS DEC), contract # C004210. Although the research described in this article has been funded in part by the US Environmental Protection Agency, it has not been subjected to the Agency's required peer and policy review and therefore does not necessary reflect the views of the Agency, and no official endorsement should be inferred. We also thank NYS DEC for providing speciation filter data. We would like to thank Queens College for cooperation and logistical support during the campaign.

Current address of Frank Drewnick: Institute of Atmospheric Physics, University of Mainz, D-55128 Mainz, Germany.

Address correspondence to Kenneth L. Demerjian, Atmospheric Sciences Research Center, SUNY Albany, 251 Fuller Road, Albany, NY 12203. E-mail: kld@asrc.cestm.albany.edu

INTRODUCTION

Atmospheric aerosols play an important role in atmospheric processes like climate forcing, heterogeneous chemistry, and cloud formation (Andreae and Crutzen 1997; Ravishankara 1997; Jacob 2000; Hizenberger et al. 1999). Their impact on human health is also a subject of increasing concern (Pope et al. 2002; Kuenzli et al. 2000; Samet et al. 2000). The enhanced interest in ambient particulate matter has resulted in a considerable increase in aerosol research efforts. Still, many questions concerning particle formation, transport, and transformation remain largely unanswered. Adequate instrumentation that is capable of providing real-time measurements of particle composition and chemically resolved size distributions is needed to offer insight into these important issues.

The $PM_{2.5}$ Technology Assessment and Characterization Study–New York (PMTACS–NY) is one of several US EPA "Supersites" intended to provide enhanced measurement data on chemical and physical composition of particulate matter and its associated precursors. One of the primary objectives of this study is to test and evaluate new measurement technologies for particulate matter through laboratory evaluation and field intercomparison studies of new and established techniques. To this end, several recently developed instruments for real-time aerosol analysis were deployed in a field intensive in New York City during July 2001.

One of the measurement technologies deployed was an aerosol mass spectrometer (AMS) developed by Aerodyne Research Inc. (Jayne et al. 2000; Jimenez et al. 2002). The AMS samples aerosol through an aerodynamic lens, (Liu et al. 1995a, b), which is used to focus and transmit particles to an impaction region where thermal desorption of the particles and

electron impact ionization of the vapor occurs prior to mass analysis by a quadrupole mass spectrometer (Allen and Gould 1981; Sinha et al. 1982). The technique provides sensitive and quantitative analysis of the volatile and semivolatile components of the sampled aerosol particles. Additionally, aerosol size distributions are determined for selected species using a particle time-of-flight measurement technique.

In this article, operational parameters, quality assurance measures, data processing strategies, and first results of aerosol mass concentration measurements obtained during the PMTACS–NY 2001 AMS deployment are reported. A companion article (Part II) presents results of size-distribution measurements performed with the AMS during this same campaign.

INSTRUMENT DESCRIPTION

A schematic of the AMS instrument is shown in Figure 1. A more detailed description is given in Jayne et al. (2000). The AMS is relatively compact, measuring 115 cm × 85 cm × 55 cm in size, including all vacuum pumps. The electronics for the quadrupole mass spectrometer, for the pumps, pressure gauge, and the data acquisition computer, fit altogether in a half rack. The total power consumption under sampling conditions is about 600 W.

The vacuum system consists of three differentially pumped chambers: an aerosol sampling chamber, a particle sizing chamber, and an analysis chamber. The three chambers are divided by a skimmer and a channel aperture, respectively. Typical pressure in the analysis chamber under sampling conditions is 1.6×10^{-6} Pa.

The ambient aerosol is introduced into the aerosol-sampling chamber through an aerodynamic particle beam-forming lens, similar to that described by Liu et al. (1995a, b). Particles in the range of approximately 50–600 nm are focused with almost 100% efficiency, allowing a quantitative analysis of most of the accumulation mode aerosol. The inlet flow is restricted to 0.1 l/min by a critical orifice of 100 μm ID in front of the lens.

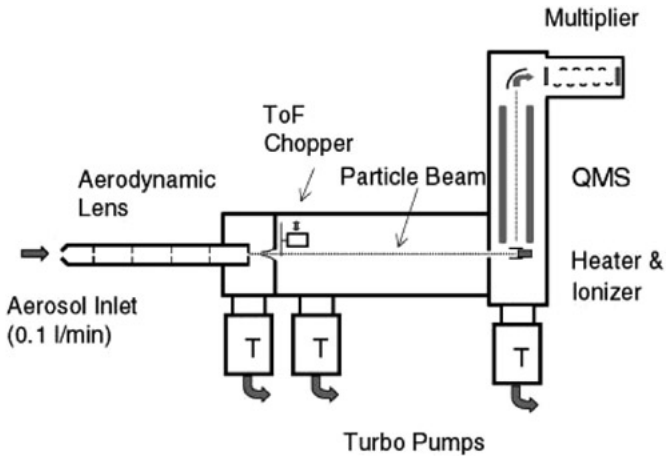

Figure 1. Schematic of AMS. Ambient aerosol is sampled and focused through the aerodynamic lens into the vacuum. The fine particle beam passes through a skimmer and (during ToF mode) a chopper and impacts onto a heater, followed by flash vaporization and electron impact ionization. The ions are analyzed by a quadrupole mass spectrometer.

After traversing the aerosol sampling chamber, the particle beam passes a skimmer and a chopper, then passes through the particle-sizing chamber of 30 cm length and an aperture, and finally impacts on a 700°C heater. The heater consists of a flat molybdenum surface covered with a molybdenum mesh. After flash vaporization of the volatile and semivolatile particle components, the vapor is ionized by electron impact, using 70 eV electrons. The ions are analyzed by a quadrupole mass spectrometer (QMS, *Balzers* QMG 422) and detected with a calibrated electron multiplier.

During this campaign the AMS heater/vaporizer was operated at a temperature of 700°C. The AMS measures only nonrefractory components of the sampled aerosol that vaporize at this oven temperature. Under the worst-case assumption that all of the refractory material remains on the heater, a layer on the order of 100 nm per day builds up under the conditions of PMTACS–NY 2001 (typical refractory aerosol concentrations taken from filter measurements). This would result in a total layer thickness of a few micrometers during the whole campaign. This layer thickness is assumed not to affect the evaporation process significantly.

The AMS operates in two different modes: The mass spec (MS) mode and the time-of-flight (ToF) mode. In the MS mode the average composition of the nonrefractory aerosol components is determined by scanning the complete mass spectrum (1–300 amu) with the QMS. Particle-size distributions are not obtained in this mode. In the ToF mode mass-weighted size distributions are determined for species that are associated with several selected fragments, by measuring the time-resolved ion signal for these fragments after chopping the aerosol beam with the chopper.

For switching between these operation modes the chopper is mounted on a slide, which can be moved in and out of the beam by a computer-controlled servo motor.

To measure the aerosol mass spectrum in the MS mode the chopper is moved completely out of the particle beam ("beam open" position). This maximizes the number of particles transmitted to the heater (100% particle transmission for spherical particles of 60 nm $< D_{aero} <$ 600 nm) in order to optimize sensitivity. In this mode the mass spectrometer is repeatedly scanned over a mass range from m/z = 1–300 amu at a frequency of 3 Hz, measuring the average bulk composition of the nonrefractory aerosol components. The instrument background signal is also routinely measured by moving the chopper wheel into the particle beam ("beam closed" position) and completely blocking particle and air access to the heater/ionization chamber. The difference between the mass spectra obtained at the beam open and beam closed positions (difference spectrum) is used for the calculation of aerosol mass concentration.

For particle sizing, the chopper wheel (2% duty cycle) is moved only a certain amount into the particle beam, so that the beam is chopped by the slit in the chopper wheel ("beam chopped" position). The chopper is located immediately following the skimmer at the beginning of the sizing chamber. During the expansion into the vacuum at the end of the aerodynamic lens the particles are accelerated according to their aerodynamic properties. In this ToF mode the quadrupole mass spectrometer is set to sample several selected masses and measure the time-resolved ion signals relative to the rotational phase of the chopper at each mass setting. These measurements yield the particle velocity distributions for the selected masses, which are converted into size distributions for the species associated with each mass.

Field Operation and Data Processing

During the PMTACS–NY 2001 summer intensive the AMS was operated at the measurement site at Queens College in Queens, New York from 30 June until 5 August. The measurement site was located at the edge of parking field #6 adjacent to an athletic field. Queens College (40.74° N, 73.82° W, altitude: ~25 m a.S.L.) is located in the heart of Queens, approximately a hundred meters south of Long Island Expressway and 1 km east of Van Wyck Expressway, two high-traffic highways in the New York City metropolitan area.

The AMS was housed in an air-conditioned trailer together with other aerosol instruments. The sampling inlet was mounted on a tower at a height of 5 m above the ground next to the trailer. The sample line from the tower to the instrument was approximately 2 m. Ambient air was sampled via a $PM_{2.5}$ cyclone (*URG* 2000-30EN) at 10 l/min and through 14.1 mm ID copper tubing. The tube diameter was chosen to minimize losses by impaction and gravitational settling for the given flow rate. The overall transport losses were calculated using simple formulas for diffusion, gravitational settling, and impaction losses (Hinds 1999) for the inlet geometry. Averaged over the size range transmitted into the AMS, the transport losses are about 1.3%. A detailed discussion of the dependence of transport losses on particle size is given in Drewnick et al. (2003b).

At the entrance of the AMS inlet, a sample flow of 0.4 l/min is isokinetically extracted from the 10 l/min transport flow. A fraction of this flow (0.3 l/min) is diverted to a CPC (*TSI* 3025) while 0.1 l/min is introduced into the AMS inlet. Due to the very low flow rate the transport losses within the first few centimeters of the AMS inlet entrance are larger for small particles than in the copper tube: The average transport loss in this part of the inlet is about 1.9%. Including the relatively small losses of the isokinetic sampling probe, the calculated range of the total inlet losses are about 11% for 20 nm and 9% for 2.5 μm particles, with a minimum of 0.7% for 350 nm particles. The unweighted average total transport losses for the particle diameter range of 20 nm to 2.5 μm are 3.5%. In the field the AMS was operated to periodically switch (i.e., 20 s cycle) between the ToF mode (size information for preselected masses) and the MS mode (complete mass spectrum for bulk aerosol).

The fragments (and associated species) chosen in the ToF mode during this campaign were: m/z = 15 amu (NH^+; ammonium); 30 and 46 amu (NO^+, NO_2^+; nitrate); 32 amu (O_2^+; air, for monitoring of the multiplier gain; see below); 48, 64, and 80 amu (SO^+, SO_2^+, SO_3^+; sulfate); and 55, 57, 69, 71, and 123 amu (organic fragments). The masses associated with organic species belong to several groups of organics. They were chosen because they were the most prominent masses in the organic fraction of the mass spectrum.

The mass spectrometer was set to a resolution slightly better than single mass unit resolution to maximize ion transmission through the mass spectrometer and prevent spillover of signal from intense lines into adjacent m/z. However, the mass spectra were recorded in the MS mode in 0.05 amu steps. These "high resolution" spectra were later converted into spectra with single mass resolution, using the center 0.4 amu of every mass peak. The MS mode was set up to switch between particle signal and instrument background signal every 5 s (15 mass scans). Every 10 min the mass spectrum and size distribution averages were saved to disc.

Since the electron multiplier gain decreases with age, it is necessary to monitor and correct for this change. Absolute calibration of the multiplier gain was performed daily by measuring the signal at the multiplier exit due to single ions produced by ionizing the background gas at lowered electron current. In addition, a continuous correction is obtained from the decrease of the oxygen signal at m/z = 32 amu (O_2^+), recorded with every mass spectrum. Since the oxygen loading should be constant and depend only on the inlet flow, which is measured independently, the multiplier gain decrease is continuously monitored using the signal at this mass.

The multiplier signal and gain, the inlet flow rate, and the efficiency of ionization and transmission of the ions through the QMS are necessary to calculate particle mass concentration. The inlet flow meter was calibrated several times in the lab before the campaign, showing no significant drifts. Ionization and quadrupole transmission efficiency calibrations were performed several times in the field. The calibration procedure involves producing ammonium nitrate particles of 350 nm mobility diameter (using a differential mobility analyzer; DMA) and introducing the particle stream into the AMS. The average number of NO_3^- ions per particle reaching the multiplier entrance is determined from the calibrated multiplier signal. The ionization and quadrupole transmission efficiency (IE) is the ratio of measured ions per particle and calculated molecules per particle. Since the NO_3^- ionization and transmission efficiency did not change significantly over the time of deployment, an average value was used (1.0e-6 ions/molecule) for the whole campaign.

The mass concentration C of a species is calculated from the multiplier signal J_f at fragment f following Jimenez et al.

(2002):

$$C = \frac{J_f \cdot M}{X_f \cdot (\mathrm{IE}) \cdot G \cdot Q}, \quad [1]$$

where M is the molecular weight of the species, X_f is the fraction of total ions generated for this species that appears at this m/z, and IE is the ionization and quadrupole transmission efficiency of the species of interest. The ionization efficiencies of species other than nitrate are expressed as a product of the regularly calibrated NO_3^- IE and a species-specific correction factor that can be measured in the laboratory (P. J. Silva 2001, Aerodyne Research, Inc. unpublished laboratory data; Jimenez et al. 2002). G is the multiplier gain corrected for decay, and Q is the inlet flow rate. In the AMS, most aerosol species are monitored at multiple signature fragments rather than at a single fragment. Thus, typically the sum of the ion signals at all monitored fragments and the fraction of the total ions from the species that are monitored are used for values of J_f and X_f in Equation (1).

For nitrate particles the mass concentration is simply the sum of the mass concentrations calculated for all fragments: m/z = 30 amu (NO^+) and m/z = 46 amu (NO_2^+). Chloride typically is measured as Cl^+ and HCl^+, considering chloride's two isotopes; this includes m/z = 35, 36, 37, and 38 amu. As a result of strong interferences with fragments of organic species, only m/z = 35 and 36 amu are used to calculate the chloride mass concentration. The chloride mass concentration is corrected for the omitted fragments by using the natural isotope ratio of ^{35}Cl and ^{37}Cl. Ammonium produces fragments at m/z = 15, 16, and 17 amu. Due to interferences at m/z = 16 and 17 from O_2^{2+}/O^+ and fragments of water, only the signal at m/z = 15 amu (NH^+) is used to calculate the ammonium signal. Laboratory studies with the AMS of ammonium fragmentation patterns indicate that the omitted fragments, as well as the relative IE of ammonium, were accounted for by multiplying the signal of m/z = 15 amu by a scaling factor of 4.27. This value and the signal intensity at m/z = 15 are used together in Equation (1) to calculate ammonium concentrations. Due to possible organic interference (e.g., from CH_3^+) at m/z = 15 amu, the use of this fragment for the calculation of ammonium loadings is less than ideal. In more recent versions of the AMS the water background has been significantly reduced, allowing the use of m/z = 16 and 17 amu for calculation of the ammonium mass concentration.

Sulfate fragments are mainly located at m/z = 18, 32, 48, 64, 65, 80, 81, 82, and 98 amu. Interferences with organic fragments at m/z = 65, 81, 82, and 98 amu, with water at m/z = 18 amu, and with oxygen at m/z = 32 amu led us to use only m/z = 48, 64, and 80 amu for the calculation of sulfate mass concentration. Laboratory experiments performed in the aerosol generation, calibration, and research facility (Hogrefe et al. 2003a) show that the sum of the ion signals from these three fragments must be multiplied by a factor of 1.515 to account for the omitted sulfate fragments; differences in the electron impact ionization efficiencies of sulfate and nitrate.

The sulfate, nitrate, and ammonium concentrations calculated according to the methods described above were systematically lower than those measured by other colocated instruments during this campaign. Previous lab (Hogrefe et al. 2003a) and field studies suggest that this type of systematic discrepancy is caused by incomplete focusing by the aerodynamic lens of internally mixed ammonium sulfate and nitrate particles onto the AMS vaporizer, since only particles that reach the vaporizer contribute to the measured ion signal—if the collection efficiency of the sampled particles onto the vaporizer is not 100%—by a factor that accounts for these collection losses. As shown in Part II of this article, the chemically speciated size distributions measured by the AMS suggest that the sulfate- and nitrate-containing aerosols are internally mixed. Thus, the correction factor needed to account for the lower collection efficiency of the mixed sulfate/nitrate particles can be estimated by comparing the AMS sulfate mass concentration with that measured by other semicontinuous instruments. It is important to note here that the correction factor determined in this way will account for both the incomplete focusing effects mentioned above and the differences in large particle inlet cutoffs between the AMS and the semicontinuous aerosol instruments. An empirically determined collection efficiency correction factor of 2.34 was used for this study by adjusting the AMS sulfate mass concentrations of the first week of operation to the Particle-into-liquid sampler with IC (PILS–IC; Weber et al. 2001) sulfate mass concentrations of the same time period. Intercomparisons between the corrected AMS sulfate concentrations and those measured by three other semicontinuous particulate sulfate instruments (Drewnick et al. 2003a) show that this factor does not change with time. A more detailed investigation of the collection efficiency correction factors is described elsewhere (Hogrefe et al. 2003a).

The water content of the particles can be estimated from the m/z = 18 amu signal (H_2O^+) after correction for the sulfate fragment at this mass. This water signal is comprised of the portion of water vapor in the ambient air reaching the ionization region of the AMS and the particle-bound water that has evaporated upon particle vaporization at the heater.

The particle–water concentration was determined by difference, subtracting the absolute ambient water vapor concentration from the total water signal. Local meteorological measurements of relative humidity, RH, and the air temperature, T, were used to calculate the absolute water vapor concentration, d_w, in the air using an empirical formula for the saturation pressure of water vapor (Bolton 1980),

$$d_w = \frac{\mathrm{RH} \cdot 6.112}{R_w \cdot (T + 273)} \cdot \exp\left(\frac{17.67 \cdot T}{243.5 + T}\right), \quad [2]$$

where R_w is the individual gas constant for water vapor (461.5 J/kgK) (Rogers and Yau 1989), d_w is in kg/m^3, and T is in °C. In a second step the concentration of the air d_{air} was calculated from the local air pressure p_{air}, using the ideal

gas law,

$$d_{\text{air}} = \frac{100 \cdot p_{\text{air}}}{R_{\text{air}} \cdot (T + 273)}, \quad [3]$$

where R_{air} is the individual gas constant for air (287 J/kgK) (Rogers and Yau 1989), d_{air} is in kg/m^3, T is in °C, and p_{air} is in mbar. Finally, that portion of the ambient air water vapor signal measured by the AMS was calculated from the ratio of water concentration and air concentration and the N_2^+ AMS signal at m/z = 28 amu:

$$\text{water}_{\text{humid}} = \frac{2}{2.5} \cdot 1.45 \cdot \frac{d_w}{d_{\text{air}}} \cdot \text{AMS}(\text{m/z} = 28 \text{ amu}), \quad [4]$$

where 2/2.5 is the ratio of the ionization cross sections of water vapor and nitrogen (Deutsch et al. 2000), and 1.45 is a factor to correct for the other air constituents that are not contained in the signal at m/z = 28 amu. Due to large water background signals it is assumed that the uncertainty of the calculated water signal is dominated by the uncertainty of the measured signal at m/z = 18 amu. We estimate this uncertainty to be on the order of 20%.

Lab experiments performed at Aerodyne Research Inc. (Silva 2001, unpublished data) indicate that the ionization efficiency of organic molecules is larger than for inorganic molecules of equal molecular weight. This is accounted for by the multiplication of all organic signals by a factor of 0.7. The total nonrefractory organic signal is calculated by adding up the signals of all m/zs of the mass spectrum larger than 11 amu except for those that arise from the fragmentation of inorganic aerosol species or from gas-phase air molecules. To avoid counting fragments of inorganic species as part of the organic signal, the mass spectra were first corrected for minor contributions of these species by using their fragmentation patterns and isotope ratios. Also, using the known composition of air, the signal at m/z = 40 and 44 amu (Ar, CO_2) were corrected for these species before they were used in the organic mass concentration calculation.

The organic fraction of the aerosol was further investigated by performing an ion-series analysis (McLafferty and Turecek 1996). For this mass spectrometric analysis technique it is assumed that organic molecules consist of a backbone R with CH_2 chains attached to it. Upon electron impact ionization they form picket fence-like mass spectra in which groups of peaks have a 14 amu separation due to fractionation at different positions in the CH_2 chains. The masses at which these peaks appear are characteristic of the R backbone of the molecule. Series with different Rs are classified in this approach according to their Δ value:

$$\Delta = \text{peak mass} - 14n + 1, \quad [5]$$

where n is the number of CH_2 groups remaining on the backbone. Different Δ groups are associated with different groups of organic species. Previous lab- and field-measurement results indicate that some of the Δ groups can be used as signatures of certain types of organic aerosol particles (M. Canagaratna 2002, personal communication): Δ = 0, 2 (m/z = 13, 27, 41, 55, ... and 15, 29, 43, 57, ... amu) correspond to traffic related aerosol; Δ = 3 (m/z = 16, 30, 44, 58, ... amu) correspond to photochemically produced particles; and Δ = −7 (m/z = 20, 34, 48, 62, ... amu) correspond to aromatics. However, no direct association between Δ groups and single-chemical species can be made.

Minimum detection limits (MDLs) were calculated for every species individually from the background signal, which was measured routinely in the MS mode by completely blocking the aerosol beam. MDLs were defined as three standard deviations of the background signal. Average 10 min detection limits for the whole campaign are 0.16 μg/m^3 for sulfate, 0.07 μg/m^3 for nitrate, 0.25 μg/m^3 for ammonium, 0.02 μg/m^3 for chloride, and 0.93 μg/m^3 for organics. The accuracy and precision of the AMS mass concentration measurements are still under investigation. This was and will be done by instrument intercomparison studies in the laboratory and in the field (e.g., Drewnick et al. 2003a; Hogrefe et al. 2003b) as well as systematic laboratory studies to investigate AMS performance (e.g., Hogrefe et al. 2003a). At this time relative uncertainties of AMS mass concentration measurements are estimated to be in the 10–20% range.

RESULTS AND DISCUSSION

The AMS performed reliably during the PMTACS–NY 2001 field campaign, leading to a rich dataset of high-frequency measurements of aerosol mass concentration and size distribution. During the campaign period, 30 June to 5 August, the AMS acquired valid data, in the form of 10 min averages, >93% of the time. One quarter of the lost time was due to calibration and regular maintenance procedures, and the remaining lost time was caused by data acquisition computer failure. No measurement time was lost due to failure of the instrument itself.

A data summary of the AMS PMTACS–NY dataset, giving minimum, median, mean, and maximum for the sulfate, organics, nitrate, ammonium, chloride, and the total nonrefractory mass concentration is presented in Table 1. Some of the minimum mass concentrations are negative due to noise in the signal at the associated masses. Even though typical (median) mass

Table 1
Data summary of the PMTACS–NY data, obtained with the AMS

	Minimum	Median	Mean	Maximum
Sulfate	0.05	2.56	3.94	53.16
Organics	−0.09	2.28	2.65	30.12
Nitrate	−0.09	0.41	0.81	10.56
Ammonium	0.01	1.09	1.41	7.44
Chloride	−0.06	0.02	0.03	0.45
Total mass	−0.07	8.10	10.60	83.11

Values in μg/m^3.

concentrations of all species are in the range below 4 $\mu g/m^3$, pollution events reported for sulfate and/or organics mass concentrations are well above 20 $\mu g/m^3$ averaged for 10 min intervals. During these events the total mass concentration were observed to reach or exceed 40 $\mu g/m^3$.

Average diurnal patterns for the entire campaign data set were calculated from the time series of the sulfate, nitrate, nonrefractory organics, and total nonrefractory aerosol mass concentrations. Figure 2 presents the diurnal data in the form of boxplots, providing the medians and 5, 25, 75, and 95% percentiles as well as the means of the mass concentrations for every hour of the day.

The results reported in Figure 2 indicate almost no diurnal pattern in the medians of the sulfate particulate mass concentration, while the mean values exhibit a small maximum during the later afternoon hours. The majority of this diurnal pattern is associated with the four most intense sulfate events, which occur on timescales of days and appear to be reflective of regional pollution episodes. The afternoon maximum during these events is likely due to in situ photochemical processing of gas-phase SO_2 in these polluted air masses, though a definitive analysis would require accounting for the detailed meteorology.

In contrast, the nitrate particle concentration has a clear diurnal pattern in the average values as well as in the median mass concentrations with a maximum in the early morning hours, peaking around 6:00 to 7:00 local time. The nitrate mass concentration decreases continuously after this time until it reaches a minimum in the late afternoon. During the night it increases

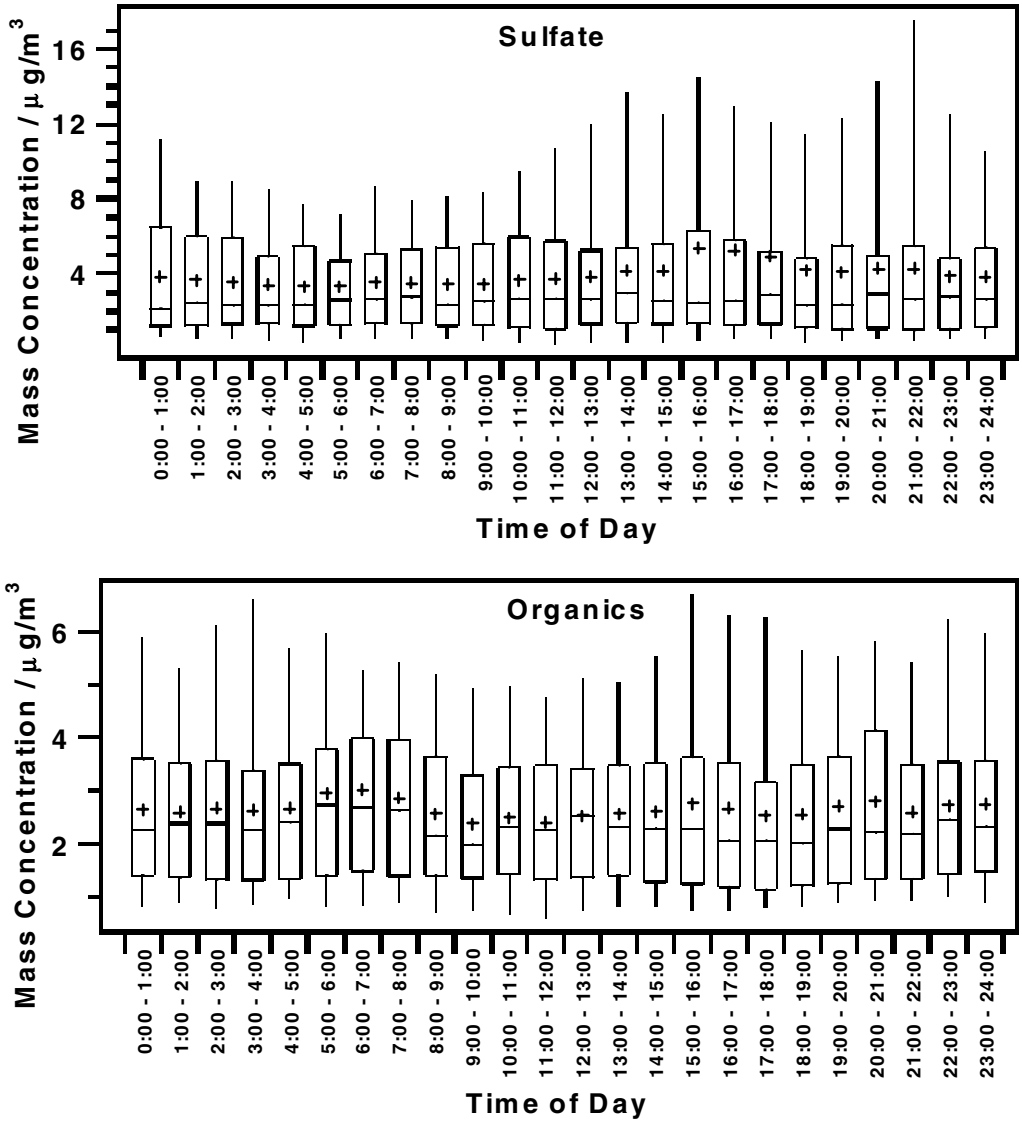

Figure 2. Average diurnal patterns for sulfate, nitrate, total organics, and total nonrefractory mass concentrations, measured during PMTACS–NY 2001. The boxes indicate the 25th percentile, the median, and the 75th percentile. The whiskers indicate the 5th and 95th percentiles. The means are printed as crosses. *(Continued)*

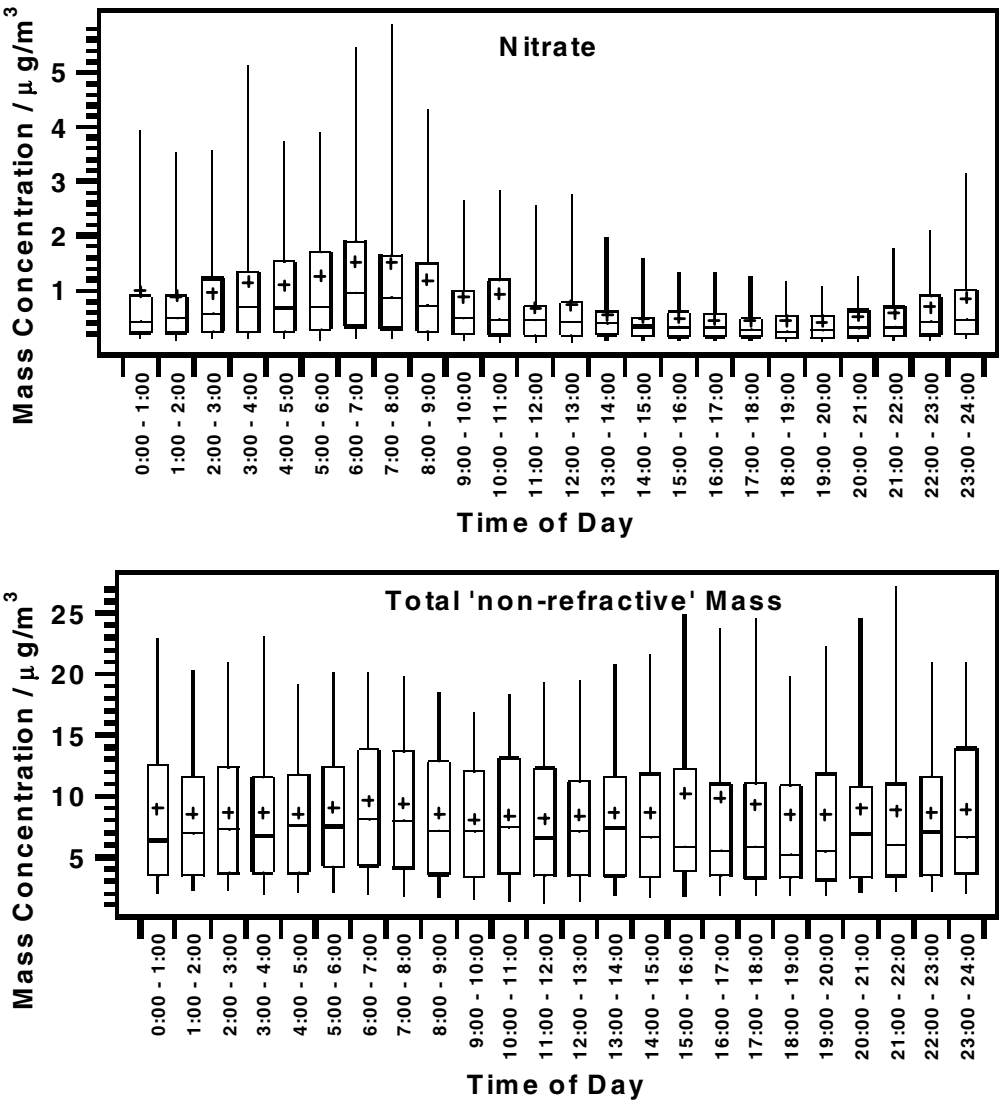

Figure 2. (Continued)

again until the early morning, with a small secondary maximum around midnight.

Ammonium nitrate (NH_4NO_3), the most likely source of the observed PM nitrate signal, is formed in an equilibrium reaction involving gas-phase nitric acid and ammonia,

$$HNO_3 + NH_3 \leftrightarrow NH_4NO_{3(s)} \qquad [6]$$

This equilibrium is very temperature sensitive, shifting towards the gas-phase species with increasing temperature (Seinfeld and Pandis 1998):

$$\ln K_p = 84.6 - \frac{24220}{T} - 6.1 \cdot \ln\left(\frac{T}{298}\right), \qquad [7]$$

with T in K.

The observed nitrate diurnal pattern is qualitatively consistent with the observed summertime diurnal temperature pattern for the measurement period. Similar diurnal patterns of nitrate partitioning were found in other measurements as well as in model calculations (Ansari and Pandis 1999).

The mass concentration of total organics also shows a measurable diurnal pattern. There is a maximum during morning rush hour, ranging from 5:00 to 8:00 for the average as well as for the median concentration. For the mean concentration there is also a maximum during the afternoon rush hour (15:00–18:00) and later in the evening (19:00–22:00). These two maxima are less clearly seen in the median values.

The total nonrefractory mass concentration shows two maxima during the day: one at the morning rush hour between 6:00 and 8:00 and one in the later afternoon between 16:00 and 18:00. These two maxima can be seen in both the mean and, to a lesser extent, in the median values.

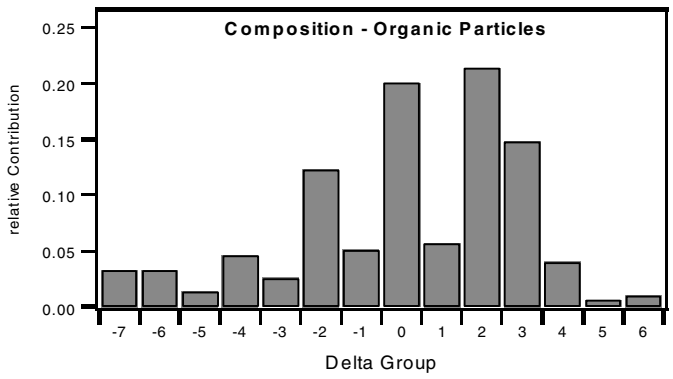

Figure 3. Average composition of the organic aerosol fraction according to the delta analysis. The relative contribution for every delta group is displayed. Delta groups 0 and 2 are related to traffic aerosol, and delta group 3 is a marker for photochemically produced particles.

In Figure 3, the average composition of the organic particles is shown by displaying the average pattern of contributions of the mass signals to the 14 Δ groups determined from ion series analysis as described in the previous section. The most prominent delta groups are the ones with $\Delta = -2$, 0, 2, and 3. Due to the nature of this approach, no delta group can be directly identified with a single species or even with a certain chemical "family," but different types of organic particles show distinct delta pattern "fingerprints." The most prominent groups in these fingerprints can be used as markers for the type of organic aerosol particles. Photochemically generated organic aerosol species, for example, give rise to AMS spectra with a prominent $\Delta = 3$ group (largely due to m/z = 44 amu from CO_2^+) and some $\Delta = 0$ and $\Delta = 2$ contributions as well. Mass spectra of traffic-related hydrocarbon species can be identified by large contributions from the $\Delta = 0$ and $\Delta = 2$ groups. Using this association it appears that a major fraction of the organic particles measured in New York City have sources associated with both traffic and photochemical processes. However, because these organic fingerprints have significant overlap among the delta groups, exact quantification of these fractions is not possible at this time.

While the average diurnal pattern of the total organics mass concentration is very weak, the fractions of the total mass spectral ion signal due to the ion-series signatures of traffic-related aerosol ($\Delta = 0$ and $\Delta = 2$) and ion-series signatures of photochemically generated aerosol ($\Delta = 3$) have a clear diurnal pattern, as shown in Figure 4. As expected, the fraction of ions corresponding to the traffic-related particle signatures shows maxima during the two high-traffic periods in the morning and the late afternoon until late night. On the other hand, the diurnal pattern of the fraction of ion-series signatures for photochemically generated particle agrees well with what one would predict, with a clear maximum during the noon and afternoon hours of maximum light intensity and a minimum during nighttime. The second local minimum during the early morning hours is simply due to the large increase in traffic-related particle signatures (maximum in left pattern) during this time, which reduces the other fractions accordingly.

In general, the diurnal patterns in the mass concentrations of the different aerosol species are not very pronounced. Weak diurnal patterns indicate that the measured aerosol is largely influenced by regional transport (i.e., the largest increases and decreases of aerosol loading occur on time scales of several days rather than in a single day). This is most clear for sulfate, which has the largest overall variability while exhibiting the weakest diurnal pattern. At the same time, the measurable diurnal variability in the relative fractional intensities of the various organic ion-series is indicative of some significant contributions by local primary and secondary particle production, likely due to the presence of large local sources around the measurement location.

The average particle-bound water mass concentration observed during the study was 0.89 μg/m^3. This determination of particulate water content is subject to at least two errors. First, due to the relatively high volatility of water, it is expected that some of the particulate water will evaporate from the particles while they are traveling through the vacuum. Water vapor that diffuses out of the particle beam will be lost in this process. Second, condensation of water vapor onto the particles, while they are traveling through the part of the inlet line exposed to the cooled trailer air, cannot be excluded.

Adding all species mass concentrations directly measured by the AMS and the calculated particle water mass concentration results in the "total nonrefractory" mass concentrations displayed in Table 1. An aerosol mass balance was estimated from comparison of the total nonrefractory mass measured by the AMS with a semicontinuous $PM_{2.5}$ measurement performed at the same site using a tapered element oscillating microbalance (TEOM) mass monitor (Rupprecht & Pataschnick Inc.; Patashnick and Rupprecht 1991). The TEOM monitor measures the total aerosol mass by recording the frequency changes of an oscillating filter element due to an increase in filter mass by particle deposition. The correlation between AMS and TEOM monitor is shown in Figure 5.

The linear correlation shown in Figure 5 between the AMS total nonrefractory mass concentration and the TEOM total mass concentration has an intercept close to zero (0.22 μg/m^3) and a correlation coefficient of $R^2 = 0.91$. The slope of the correlation function is 0.59. For comparison of the relative efficiency of aerosol measurement of the AMS with the TEOM Monitor, the "recovery" of the AMS measurement was calculated as the slope of the correlation between these instruments with the intercept forced to zero. This recovery is 0.62, indicating that the AMS "sees" about 62% of the total aerosol mass measured by a TEOM.

The average AMS aerosol composition over the whole campaign is displayed in Figure 6. A comparison between the average AMS total nonrefractory mass for the whole campaign and the average TEOM total mass leads to a slightly different

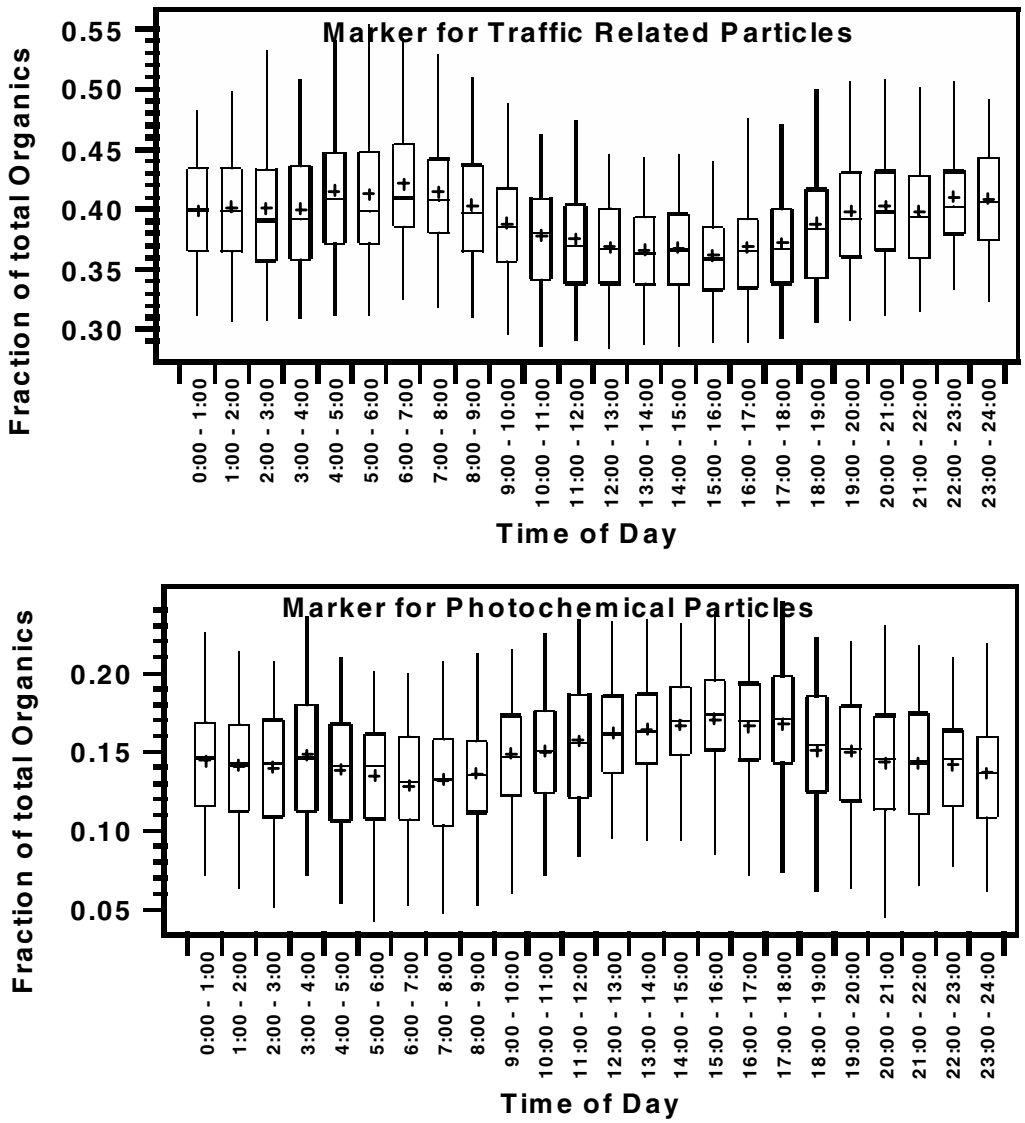

Figure 4. Average diurnal patterns of the fraction of organic particles, identified as markers for traffic aerosol and for photochemical aerosol. Unlike the diurnal pattern of the total organic mass concentration, these fractions both show a distinct diurnal pattern.

"recovery" for the AMS: according to this average the AMS was capable of identifying 64% of the total aerosol mass measured by the TEOM Monitor (patterned pieces in the pie chart).

The AMS measurements indicate that an average of 25% of the measured TEOM total aerosol mass concentration can be attributed to sulfate; nonrefractory organics account for approximately 18% and ammonium accounts for about 9% of the total TEOM mass. Nitrate mass concentrations, which were quite low during this campaign, account for only 5.5% of the total mass on average. Even less chloride was found in the particles. Approximately 6% of the total mass is assigned to particulate water. It should be noted that particle-bound water is lost in both instruments. The TEOM monitor is either equipped with a dryer or operates at 50°C to evaporate particulate water (both versions were deployed during the campaign and are reflected by the TEOM data used here). In the AMS the particles travel through the vacuum for several milliseconds before they impact on the heater. During this time some surface water will also evaporate from the particles as indicated above. The fraction of the surface water that survives the evaporation processes in both instruments is not known.

About 36% of the aerosol mass, as measured by the TEOM, was not measured by the AMS using the mass concentration calculation and correction procedures as described above (solid pieces, moved out of pie chart in Figure 6). In general, AMS measurements of aerosol mass are expected to be smaller than TEOM total mass measurements because the AMS does not

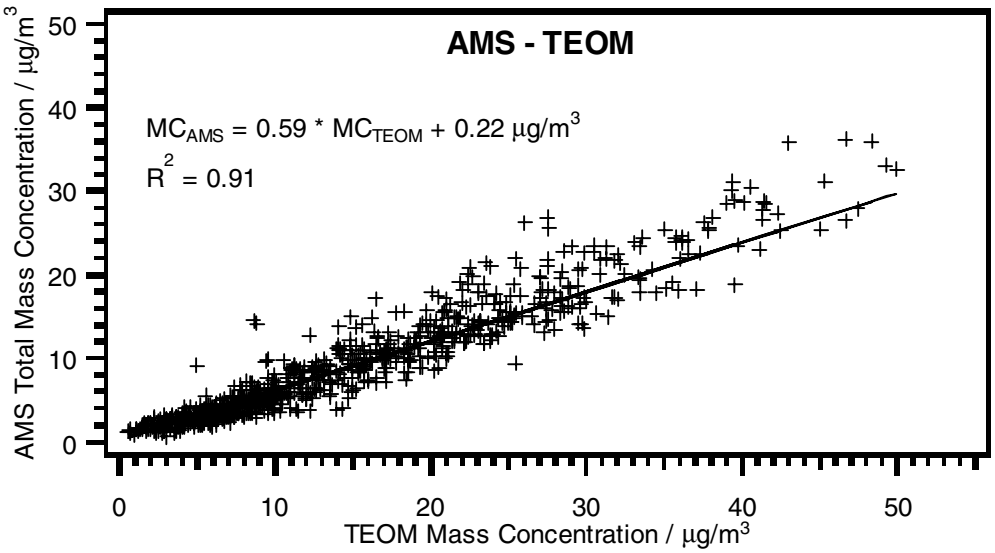

Figure 5. Correlation between AMS total nonrefractory mass and TEOM total aerosol mass concentration.

measure refractory aerosol components. The refractory aerosol components not measured by the AMS include metals and elemental carbon. According to XRF measurements of Teflon filter samples collected during this campaign, the average metal fraction of the total $PM_{2.5}$ aerosol mass is 2.1%. The mass concentration of elemental carbon (EC) was determined from Quartz filters, using NIOSH method 5040. The average EC fraction of $PM_{2.5}$ for the filters collected during this campaign was 1.8%. The sampling efficiency of the AMS aerodynamic lens drops off sharply for particles with aerodynamic diameters larger than 600 nm. Thus, the agreement between the AMS and TEOM mass measurements will depend on the fraction of the total TEOM particle mass that is present in the 600 nm to 2500 nm diameter range. Although this information is not directly available because no independent size-resolved measurements of the aerosol chemical composition (e.g., micro orifice uniform deposition impactor (MOUDI) measurements) were performed during this study, some information about it can be indirectly obtained by comparing the measurements of four semicontinuous particulate sulfate instruments with several sets of $PM_{2.5}$ filter sulfate measurements (Drewnick et al. 2003a). These intercomparisons reveal that while the semicontinuous instruments agree very well with each other, their sulfate mass concentrations are about 15% smaller than sulfate mass concentrations measured from the filter samples. While some of this difference is due to varying inlet line losses between the semicontinuous and filter experiments, the majority of this discrepancy is due to a combination of differences in the $PM_{2.5}$ selector cutoffs and incomplete sampling of $PM_{2.5}$ by the semicontinuous instruments (Drewnick et al. 2003a). The AMS sulfate mass concentrations, after correction for aerodynamic lens collection losses, agree well with the other semicontinuous sulfate instruments. This suggests that 15% of the calculated AMS sulfate mass is also "lost" due to incomplete $PM_{2.5}$ sampling. Since the sulfate, ammonium, and nitrate components of the sampled aerosols appear to be internally mixed (See Part II of this article), 15% of each of the calculated AMS ammonium and nitrate mass concentrations is "lost" as well. As shown in the pie chart in Figure 6, the sum of all this "lost" inorganic mass accounts for 6% of $PM_{2.5}$ as measured by the TEOM monitor.

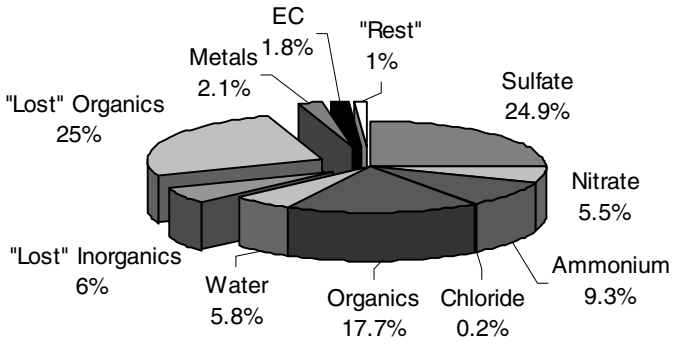

Figure 6. Average aerosol composition during PMTACS–NY 2001 as measured by the AMS. The total aerosol mass ($PM_{2.5}$) was given by TEOM measurements. The AMS was capable of identifying approximately 64% of the total aerosol (patterned pieces). The remaining 36% of the total aerosol mass is attributed to refractory aerosol components (metals, elemental carbon) not measured by the AMS, as well as transport, inlet, and focusing losses for sulfate, nitrate, ammonium, and organics not otherwise accounted for.

For the organic particulate mass concentration no reliable comparison exists to make a serious attempt at correcting for the losses due to incomplete transmission and lens focusing. According to AMS measurements of the size distributions of the organics (Drewnick et al. 2003b) an average of 84% of the organic mass concentration (as measured by the AMS) is

located in the accumulation mode. The remaining 16% is located in the small particle mode with diameters below 120 nm. Under the assumption that the organic particles in the accumulation mode show the same transport, transmission, and focusing losses as the sulfate particles in this size range, the "organics" fraction measured by the AMS also has to be corrected by applying the correction factor for sulfate losses (2.34) and for the 15% loss observed for the semicontinuous sulfate instruments compared to the filter data. The *lost organics* fraction calculated using these assumptions accounts for 24.4% of the total $PM_{2.5}$ mass concentration and is also displayed in Figure 6.

Together with the measured mass concentrations this process of estimating both of the refractory components not measured by the AMS and the lost fractions of $PM_{2.5}$ not sampled by the AMS accounts for 99% of the observed TEOM mass. The rest of the 1% of the TEOM mass that is unaccounted for is well within the relative errors of the calculated mass concentrations.

In addition to this average aerosol composition we are able to provide a semicontinuous mass balance for the whole campaign, obtained by adding up all species measured by the aerosol mass spectrometer, as displayed in Figure 7. Figure 7 shows a synoptic behavior of the aerosol concentration during this summer period, that is, relatively clean periods lasting a few days up to a week, followed by pollution events of several days mainly dominated by sulfate aerosol. These patterns are currently under study and will be presented in future work.

SUMMARY AND OUTLOOK

An aerosol mass spectrometer (AMS) was deployed in Queens/New York during the PMTACS–NY 2001 summer campaign providing 10 min averages of sulfate, nitrate, ammonium, chloride, and total organics mass concentration data almost continuously over a period of more than five weeks.

Very little average diurnal variation was observed in the reported sulfate mass concentrations. This indicates that the observed sulfate was primarily due to regional transport rather than local production. Diurnal patterns of nitrate mass concentrations show a distinct maximum at the early morning hours, which is assumed to be a result of the diurnal temperature trends.

While diurnal patterns of total organics and total nonrefractory mass concentrations show only weak maxima during morning and afternoon/evening rush-hour times, the fractions of the organic aerosol associated with traffic-related particles and photochemically generated particles show very clear diurnal patterns with maxima during high-traffic times for the traffic particles and a maximum during afternoon hours for the photochemical particles. These findings indicate that the organic particle fraction is significantly influenced by local sources, which also affects the total aerosol mass loading.

Calculated ambient water vapor concentrations from local meteorological data were used to determine the particle-bound water concentration from the AMS mass spectrum information. According to these calculations the average particle-bound water concentration during the campaign was 0.89 $\mu g/m^3$.

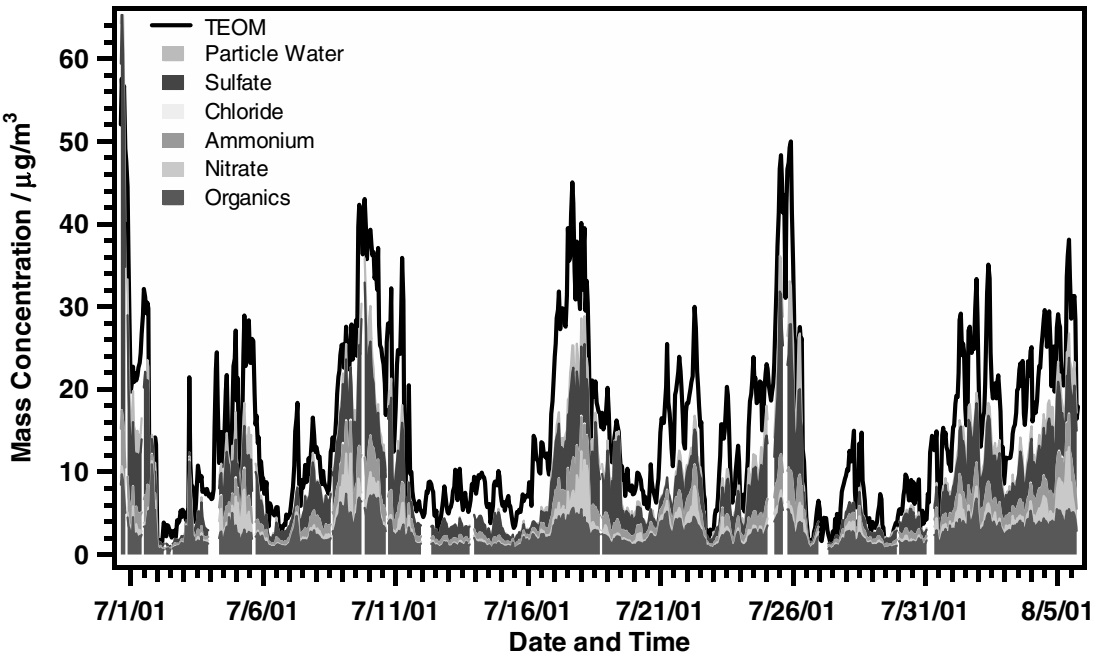

Figure 7. Semicontinuous mass balance for PMTACS–NY 2001. All species measured by the aerosol mass spectrometer. Total aerosol mass concentration measured with TEOM mass monitor. The white area between the AMS mass concentration and the TEOM mass concentration contains the refractory aerosol components as well as the "lost" inorganic and organic fractions not accounted for in the mass concentration calculations.

The total nonrefractory mass, the total mass concentration of all species identified by the AMS including particle water, was compared to the total $PM_{2.5}$ mass concentration measured by a TEOM mass monitor at the same site. In this comparison a very good correlation with an intercept close to zero and a correlation coefficient of $R^2 = 0.91$ was found between the AMS and the TEOM monitor mass concentrations.

On average the AMS identified 64% of the total mass measured by the TEOM monitor using the calculation procedures described above. Using comparisons between semicontinuous instruments and filter data, performed for data collected during this campaign, as well as filter data on the refractory aerosol mass concentration, 35% of the remaining 36% can be explained and attributed to transport, transmission, and focusing losses in the AMS inlet and to refractory aerosol components. This allows a mass closure well within the uncertainties of the AMS mass concentration measurements of approximately 5–10%.

Of the aerosol detected by the AMS, the largest single fraction of the aerosol during the campaign was sulfate with ~39% (25% of the total mass). Organics accounted for the second largest fraction with more than 28% (18% of TEOM Monitor), while nitrate was a minor component with about 8.5% (5.5%). Approximately 9% (6%) of the aerosol mass was assigned to particle-bound water. Future analysis work is underway, including the comparison of the AMS mass concentration and size distribution data with other colocated instruments and case studies of selected meteorological/air pollution events.

REFERENCES

Allen, J., and Gould, R. K. (1981). Mass Spectrometric Analyzer for Individual Aerosol Particles, *Rev. Sci. Inst.* 52:804–809.

Ansari, A. S., and Pandis, S. N. (1999). An Analysis of Four Models Predicting the Partitioning of Semivolatile Inorganic Aerosol Components, *Aerosol Sci. Technology* 31:129–151.

Andreae, M. O., and Crutzen, P. J. (1997). Atmospheric Aerosols: Biogeochemical Sources and Role in Atmospheric Chemistry, *Science* 276:1052–1058.

Bolton, D. (1980). The Computation of Equivalent Potential Temperature, *Monthly Weather Rev.* 108:1046–1053.

Deutsch, H., Becker, K., Matt, S., and Märk, T. D. (2000). Theoretical Determination of Absolute Electron-Impact Ionization Cross Sections of Molecules, *Int. J. Mass Spect.* 197:37–69.

Drewnick, F., Jayne, J. T., Canagaratna, M., Worsnop, D. R., and Demerjian, K. L. (2004). Measurement of Ambient Aerosol Composition During the PMTACS-NY 2001 Using an Aerosol Mass Spectrometer. Part II: Chemically Speciated Mass Distributions, *Aerosol Sci. Technol.* 38:104–117.

Drewnick, F., Schwab, J. J., Hogrefe, O., Peters, S., Husain, L., Diamond, D., Weber R., and Demerjian, K. L. (2003a). Intercomparison and Evaluation of Four Semi-Continuous PM-2.5 Sulfate Instruments, *Atmos. Environ.* 37:3335–3350.

Hinds, W. C. (1999). *Aerosol Technology*, 2nd ed. Wiley Interscience, New York.

Hizenberger, R., Berner, A., Giebl, H., Kromp, R., Larson, S. M., Rouc, A., Koch, A., Marischka, S., and Puxbaum, H. (1999). Contribution of Carbonaceous Material to Cloud Condensation Nuclei Concentrations in European Background (Mt. Sonnblick) and Urban (Vienna) Aerosols, *Atmos. Environ.* 33:2647–2659.

Hogrefe, O., Drewnick, F., Schwab, J. J., Peters, S., Diamond, D., Weber, R., and Demerjian, K. L. (2003b). Intercomparison and Performance Evaluation of Semi-Continuous PM-2.5 Nitrate Instruments during the PMTACS-NY Summer 2001 Campaign in New York City, *Atmos. Environ.* submitted.

Hogrefe, O., Drewnick, F., Lala, G. G., Schwab, J. J., and Demerjian, K. L. (2004). Development, Operation and Applications of an Aerosol Generation, Calibration and Research Facility, *Aerosol Sci. Technol.* 38:196–214.

Jacob, D. J. (2000). Heterogeneous Chemistry and Tropospheric Ozone, *Atmos. Environ.* 34:2131–2159.

Jayne, J. T., Leard, D. C., Zhang, X., Davidovits, P., Smith, K. A., Kolb, C. E., and Worsnop, D. R. (2000). Development of an Aerosol Mass Spectrometer for Size and Composition Analysis of Submicron Particles, *Aerosol Sci. Technol.* 33:49–70.

Jimenez, J. L., Jayne, J. T., Shi, Q., Kolb, C. E., Worsnop, D. R., Yourshaw, I., Seinfeld, J. H., Flagan, R., Zhang, X., Smith, K. A., Morris, J., and Davidovits, P. (2003). Ambient Aerosol Sampling Using the Aerodyne Aerosol Mass Spectrometer, *J. Geophys. Res.—Atmos.* 108:8425.

Kuenzli, N., Kaiser, R., Medina, S., Studnicka, M., Chanel, O., Filliger, P., Herry, M., Horak Jr., F., Puybonnieux-Texier, V., Quenel, P., Schneider, J., Seethaler, R., Vergnaud, J.-C., and Sommer, H. (2000). Public-Health Impact of Outdoor and Traffic-Related Air Pollution: A European Assessment, *The Lancet* 356:795–801.

Liu, P., Ziemann, P. J., Kittelson, D. B., and McMurry, P. H. (1995a). Generating Particle Beams of Controlled Dimensions and Divergence: I. Theory of Particle Motion in Aerodynamic Lenses and Nozzle Expansions, *Aerosol Sci. Technol.* 22:293–313.

Liu, P., Ziemann, P. J., Kittelson, D. B., and McMurry, P. H. (1995b). Generating Particle Beams of Controlled Dimensions and Divergence: II. Experimental Evaluation of Particle Motion in Aerodynamic Lenses and Nozzle Expansions, *Aerosol Sci. Technol.* 22:314–324.

McLafferty, F. W., and Turecek, F. (1996). *Interpretation of Mass Spectra*. University Science Books, Herndon.

Patashnick, H., and Rupprecht, E. G. (1991). Continuous PM-10 Measurements Using the Tapered Element Oscillating Microbalance, *J. Air Waste Manag. Assoc.* 41:1079–1083.

Pope, C. A., Burnett, R. T., Thun, M. J., Calle, E. E., Krewski, D., Ito, K., and Thurston, G. D. (2002). Lung Cancer, Cardiopulmonary Mortality, and Long-Term Exposure to Fine Particulate Air Pollution, *J. Am. Med. Assoc.* 287:1132–1141.

Ravishankara, A. R. (1997). Heterogeneous and Multiphase Chemistry in the Troposphere, *Science* 276:1058–1065.

Rogers, R. R., and Yau, M. K. (1989). *A Short Course in Cloud Physics,* 3rd ed. Pergamon, New York.

Samet, J. M., Dominici, F., Curriero, F. C., Coursac, I., and Zeger, S. L. (2000). Fine Particulate Air Pollution and Mortality in 20 U.S. Cities, *New Engl. J. Med.* 343:1742–1749.

Sinha, M. P., Giffin, C. E., Norris, G. G., Estes, T. J., Vilker, V. L., and Friedlander, S. K. (1982). Particle Analysis by Mass Spectrometry, *J. Colloid and Interface Sci.* 87:140–153.

Seinfeld, J. H., and Pandis, S. N. (1998). *Atmospheric Chemistry and Physics.* John Wiley & Sons, Inc., New York.

Weber, R. J., Orsini, D., Daun, Y., Lee, Y.-N., Klotz, P. J., and Brechtel, F. (2001). A Particle-into-Liquid Collector for Rapid Measurement of Aerosol Bulk Chemical Composition, *Aerosol Sci. Technol.* 35:718–727.